Correspondence to:
R. Hu,
rhu@hhu.edu.cn

A Numerical Study of Slug Tests in a Three-Dimensional Heterogeneous Porous Aquifer Considering Well Inertial Effects

Quan Liu[1] , Linwei Hu[2], Peter Bayer[3], Yixuan Xing[1], Pengxiang Qiu[1], Thomas Ptak[1], and Rui Hu[4]

[1]Geoscience Center, University of Göttingen, Göttingen, Germany, [2]Institute of Geosciences, Kiel University, Kiel, Germany, [3]Applied Geology, Martin Luther University Halle-Wittenberg, Halle, Germany, [4]School of Earth Sciences and Engineering, Hohai University, Nanjing, China

Abstract The slug test is a common field technique for obtaining local hydraulic parameters near wells, applied, for example, for the hydrogeological investigation at contaminated sites. Although many slug test models have been developed for interpretation of measurements, only a few of them have considered heterogeneous conditions, and water column inertial effects are usually neglected. In this paper, we propose a novel three-dimensional slug test model (3DHIM) for application in heterogeneous aquifers, considering inertial effects associated with skin effects and linear friction forces. After comparison with existing analytical and numerical solutions of slug tests, the model is applied to an aquifer analog to simulate a series of slug tests. The results from single-well slug tests show that the well geometry (i.e., the well radius, well depth, and screen length) has an impact on the water level response. For cross-well slug tests, the results indicate that the water level fluctuations not only include information on the hydraulic signal propagation process in the aquifer but also on well characteristics, such as wellbore storage and inertial effects. These effects cause a phase shift and amplitude change of the water level fluctuation. As the observation and test wells have a good hydraulic connection and similar well geometry, the water level amplitude could be amplified relative to aquifer pressure at the measured position. Therefore, we suggest considering wellbore storage and in-well inertial effects in slug test-based subsurface investigations, otherwise the parameter estimates based on well water levels may include errors, particularly in highly permeable layers.

1. Introduction

Heterogeneity of aquifer hydraulic properties has a crucial impact on groundwater flow and solute transport. To characterize this heterogeneity, some innovative aquifer testing configurations have been developed, such as multilevel and cross-well tomographical hydraulic tests. The slug test is one of the most common approaches for obtaining local hydraulic parameters. It is based on recording the recovery of the water level in a well after an instantaneous extraction (or injection) of a certain amount of water or gas. The recovery curve contains information about the hydraulic properties of the aquifer, such as hydraulic conductivity and specific storage, which can be obtained by some inversion methods. Recently, this method has been widely used for contaminated site surveys as it requires no additional water injection or extraction. Moreover, compared to other approaches, such as those based on pumping tests, a slug test has considerable logistic and economic advantages, and it can resolve a higher degree of aquifer heterogeneity due to its small sampling scale (i.e., the volume of the subsurface sampled by a slug test). In the last decades, variants of slug test configurations for the characterization of aquifer heterogeneity have been studied (Brauchler et al., 2010; Cardiff et al., 2011; Wang et al., 2018; Widdowson et al., 1990; Zlotnik & McGuire, 1998). Tomographic slug tests, for instance, measure hydraulic head responses in the testing and observation intervals at different depths to estimate the spatial heterogeneity of the hydraulic properties between two or more wells.

In order to resolve the spatial heterogeneity of hydraulic parameters, a slug test model is usually required to establish mathematical relationships between the field test data and the parameters sought. Based on different types of slug tests, the basic options for aquifer characterization are as shown in Figure 1.
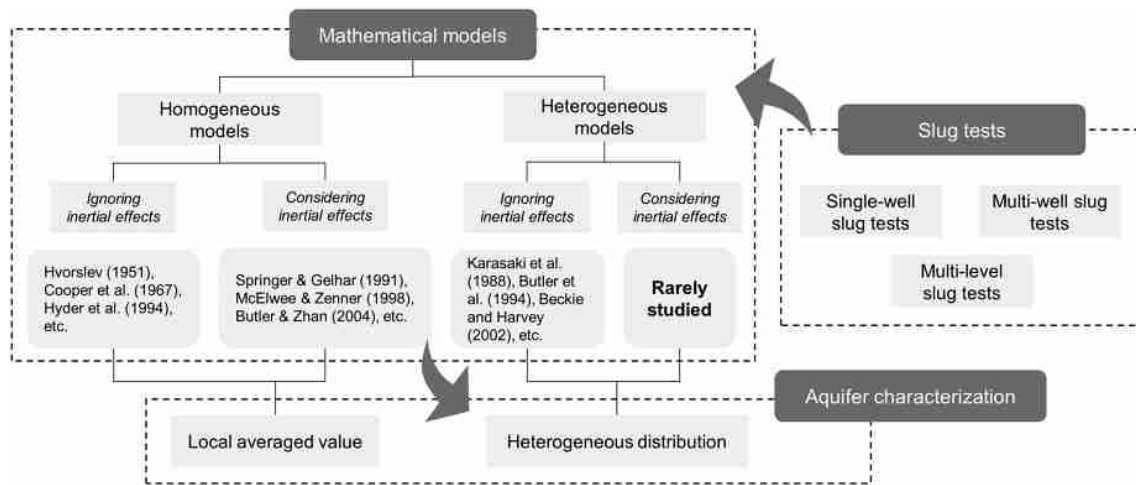
Figure 1. The basic options of aquifer characterization based on slug tests.

Among the presented slug test models, however, only a few consider heterogeneity. Karasaki et al. (1988) examined slug-induced flow in a two-layer aquifer by using an analytical model. Shapiro and Hsieh (1998) extended the Karasaki et al. model to n layers. Some numerical models were also developed to study some more complicated situations, such as multilevel slug tests. Originally, numerical models were used to analyze the tests results to obtain information on the heterogeneity of hydraulic conductivity in vertical direction (Braester & Thunvik, 1984; Butler et al., 1994; Melville et al., 1991; Widdowson et al., 1990). In these models, aquifers are conceptualized as a series of regular homogeneous layers. To establish a more realistic representation, also models with more complicated spatial heterogeneity description were proposed. Beckie and Harvey (2002) used a randomly generated transmissivity field to assess the impact of hydraulic parameter heterogeneity on the slug test results. Brauchler et al. (2007) and Paradis et al. (2015) simulated a series of synthetic tomographic slug tests by using the heterogeneous models and evaluated their inversion algorithms. All these numerical models consider hydraulic conductivity variations in horizontal or vertical directions. However, most of them focus merely on the groundwater flow in the aquifer and ignore the hydrodynamic processes inside the well.

In fact, inertia-induced oscillations of the water level in a well are not uncommon during slug tests, especially in highly permeable aquifers. This phenomenon has been extensively studied in homogeneous aquifers. Some researches point out that the magnitude of the oscillation will increase as the hydraulic conductivity of the aquifer and the water column height increase (Bredehoeft et al., 1966; Butler & Zhan, 2004). Since Bredehoeft et al. (1966) discussed the role of water-column inertia in hydraulic tests, many researchers also considered inertial effects in their analytical slug test models to interpret the oscillatory head (Butler & Zhan, 2004; Kabala et al., 1985; Kipp, 1985; Malama et al., 2011, 2016; McElwee & Zenner, 1998; Springer & Gelhar, 1991; Zurbuchen et al., 2002). Butler and Zhan (2004) presented a homogeneous slug test model for confined aquifers which considers inertial mechanisms both in the observation and test wells. Malama et al. (2016) further developed the model for unconfined aquifers. Considering the inertial effects in both wells makes their model more adequate for interpreting cross-well slug tests. Given the often-rapid oscillatory nature of water level response, the pressure transducer measured head in an accelerating water column cannot be directly related to the water level by the standard equations for calculating the height of water above the measurement point, since it involves significant accelerations in the water column. To handle this, several correction models that reduce the error between actual water level and the measured head have been proposed (McElwee, 2002; Zurbuchen et al., 2002).

To date, few studies have incorporated inertial effects into a heterogeneous slug test model. A major hurdle is the limited applicability of analytical models to represent heterogeneity. In contrast, for the common numerical methods, such as finite element and finite difference methods, a fixed solution domain is required. With these, it is challenging to simulate the oscillatory water level in the well, because it is a deforming domain problem. As remedy, the arbitrary Lagrangian-Eulerian (ALE) method was proposed (Brindt &
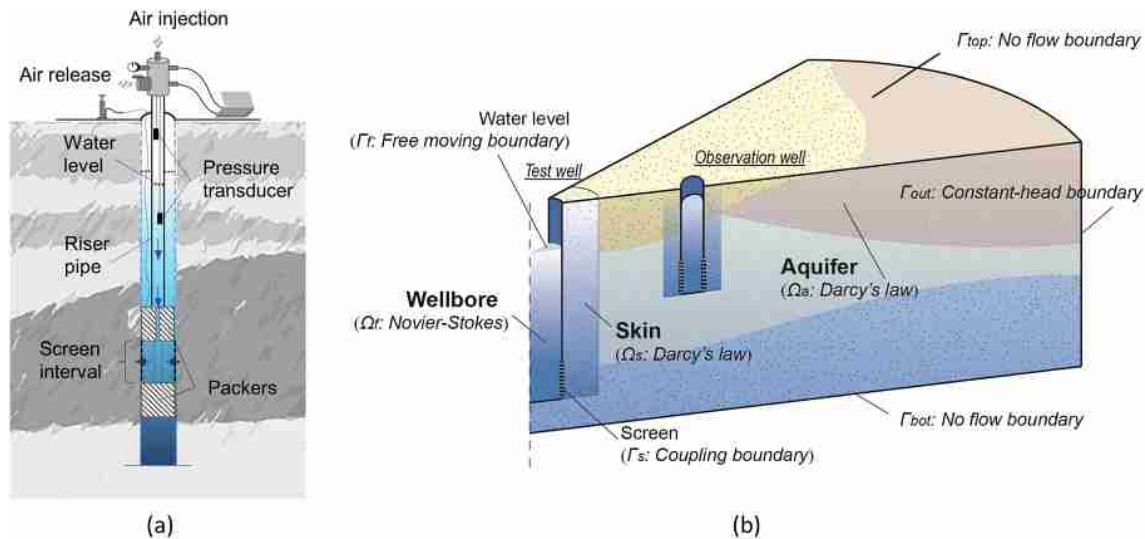
Figure 2. Schematic sketch of (a) the setup of a pneumatic slug test, and (b) a conceptual model of a slug test in 3-D heterogeneous porous formations including skin. Model settings of the test well and the observation well are the same.

Wallach, 2017; Jin et al., 2014). The ALE method combines the advantages of Eulerian and Lagrangian descriptions, which allows the computational mesh to move arbitrarily inside the domain to optimize the shapes, and which precisely tracks the material interface on the boundaries of the domain. Except for the deforming domain, interface conditions between the well and the aquifer are also not readily specifiable. Because the water flow in the well and in the aquifer is commonly represented by different physical equations, the dependent variables from different governing equations require specific continuous conditions for coupling. This coupling issue has been widely explored in many fields, such as geoscience, applied mathematics, and chemical engineering (Alazmi & Vafai, 2001; Cimolin & Discacciati, 2013; Cooper et al., 1965; Hanspal et al., 2009). Here constraints of normal stress, normal velocity, or some other specific conditions are employed to ensure the continuity of variables between different physical equations. Obviously, it is challenging, but necessary to establish a coupled numerical slug test model that accounts for both inertial effects and aquifer heterogeneity. The objective of our work is to establish a fully coupled model considering aquifer heterogeneity and inertia-controlled water level oscillations in wells.

In this study, we introduce a new three-dimensional (3-D) numerical slug test model (3DHIM) considering the inertial effects in a heterogeneous aquifer. In the following, model validation is addressed by comparing simulation results with some existing solutions. Furthermore, we examine the performance of the model by implementing an aquifer outcrop analog with a high resolution of heterogeneity. A series of single-well slug tests with different well geometry and cross-well slug tests are simulated to examine the influence of inertial effects on the slug test results.

2. Slug Test Modeling in a Heterogeneous Aquifer

2.1. Slug Test Processes in the Well-Aquifer System

Figure 2a shows the principle of a commonly used pneumatic slug test setup. After a certain amount of gas is injected into the well pipe, the water level in the riser pipe moves down until it is stable. The air pressure is then instantaneously released by opening the venting valve of the injection unit, and the air pressure is recorded by the upper pressure transducer. The recovery of the water level is recorded by the lower pressure transducer placed at a predefined depth of the water column. In fact, fluctuation of the water level can be akin to a damped simple harmonic motion (Kabala et al., 1985; Marschall & Barczewski, 1989). The main difference is that the damping effect in slug tests is controlled by the interaction of the well and the aquifer. In shallow formations of a low hydraulic conductivity, the recovery curve of the water level typically shows an overdamped behavior. That is, the water monotonically recharges to the well (or discharges to the aquifer). On the contrary, in deep and highly permeable aquifers, the recovery curve can show oscillations

with an underdamped behavior. In the latter case, the groundwater exchanges alternatively between the well and the aquifer. However, in both cases, the hydrodynamic process is always controlled by two mechanisms. One is the groundwater flow inside the well, and the other one is the groundwater flow in the aquifer. A conceptual model with the boundary types of a slug test is shown in Figure 2b. In this model, a two-dimensional (2-D) axisymmetric wellbore (Ω_f) with a moving water level boundary (Γ_f) is embedded in a 3-D heterogeneous aquifer (Ω_a), and the skin (Ω_s) is also included. The interface boundary (Γ_s) between the fluid flow and porous media flow, i.e., the well screen, is identified by certain coupling boundary conditions. No-flow boundary conditions are imposed to the aquifer top and bottom (Γ_{top} and Γ_{bom}). The outer edge of the entire model (Γ_{out}) is represented by a constant-head boundary. An observation well can be also considered, model settings of the test well and the observation well are the same. Packers are commonly used in both the test and the observation wells for multiwell slug tests. In the 3DHIM model, the wells with a double packer system (Figure 2a) are simplified to a setup only containing a corresponding screen interval and the riser pipe.

2.2. Well-Aquifer Coupling Slug Test Model

The hydrodynamic processes in the well include water exchange between the well and the aquifer, momentum dynamics of the water column in the riser pipe, and head losses due to friction within the well screen and riser pipes (Clemo, 2010; Houben, 2015; Quinn et al., 2018; Zurbuchen et al., 2002). Among them, the former two are the main processes affecting the water level fluctuation. In heterogeneous formations, a double-packer system is often utilized to isolate the well into several test intervals, which leads to a diameter change from the screen interval to the riser pipe (Figure 2a). Narrowing and enlargement of the pipe diameter at the connections between the screen interval and the riser pipe make the momentum dynamics of the water column more complicated (Zenner, 2008; Zlotnik & McGuire, 1998).

The model presented in this paper considers the abovementioned issues through a well-aquifer coupling. Besides, we also include the head losses caused by linear friction forces in the well screen and riser pipe in this model.

2.2.1. Governing Equations

2.2.1.1. Groundwater Movement Inside the Well

The movement of groundwater inside a well is affected by inertial effects. To describe this nonlinear hydrodynamic process, many different forms of momentum conservation equations were developed (Butler & Zhan, 2004; Cooper et al., 1965; McElwee & Zenner, 1998; Van der Kamp, 1976). In slug tests, the vertical motion of the water column is also significant. Accounting for the hydrodynamic behavior caused by variable well diameters, radial flow also needs to be considered. Assuming that the tangential velocity is negligible, groundwater flow in the well can be treated as 2-D axisymmetric. In some studies, the incompressible Navier-Stokes (NS) equation was adopted to describe the motion of the water column in the wellbore (Kim, 2003; McElwee & Zenner, 1998), and the friction force in the well screen and riser pipes is assumed to be linearly proportional to the vertical velocity of the water column following the Poiseuille law (Butler, 2002; Butler & Zhan, 2004; Quinn et al., 2018). Accordingly, the fluid flow rate $\boldsymbol{v_f}(r, z)$ and pressure p_f should satisfy the NS momentum and the continuity equations, reading as

$$\rho\left[\frac{\partial \boldsymbol{v_f}}{\partial t} + (\boldsymbol{v_f} \cdot \nabla)\boldsymbol{v_f}\right] = -\nabla \cdot T\left(\boldsymbol{v_f}, p_f\right) + \rho g k + \boldsymbol{f}_{fric}, \tag{1}$$

$$\nabla \cdot \boldsymbol{v_f} = 0, \tag{2}$$

where $T(\boldsymbol{v_f}, p_f) = -p_f \boldsymbol{I} + \mu(\nabla \boldsymbol{v_f} + (\nabla \boldsymbol{v_f})^T)$ is the Cauchy stress tensor, $\boldsymbol{I}$ is the identity tensor, and μ denotes the fluid dynamic viscosity. ρ is the fluid density, g is gravitational acceleration, and k is the unit vector in z-direction. ∇ and $\nabla \cdot$ are the gradient and divergence operators with respect to the coordinate system. $\boldsymbol{f}_{fric}$ represents the Poiseuille friction term, which is defined as $8\mu \boldsymbol{v_z}/r^2$. $\boldsymbol{v_z}$ is the vertical component of the fluid flow rate $\boldsymbol{v_f}$, and r is the pipe radius. For detailed derivation of Equation 1, please see the Appendix A.

2.2.1.2. Groundwater Flow in a Heterogeneous Aquifer

Darcy's law and a mass conservation equation are usually used to describe groundwater flow through an aquifer and skin. In a 3-D heterogeneous media, this can be written as

$$\mathbb{S}_\mathbb{S}\frac{\partial h}{\partial t} + \nabla \cdot \boldsymbol{v_p} = Q_m, \tag{3}$$

$$\boldsymbol{v_p} = -\mathbb{K}\nabla h, \tag{4}$$

where $\boldsymbol{v_p}$ is the Darcy velocity. h denotes the hydraulic head, which is defined as $h = z + p_m/\rho g$. p_m is the pressure in the aquifer, and Q_m is a source/sink term. $\mathbb{K}$ and $\mathbb{S}_\mathbb{S}$, which are spatially dependent, represent the hydraulic conductivity tensor and specific storage of the porous media, respectively.

Previous slug test studies revealed that the head in the test well is much less sensitive to aquifer storativity than to transmissivity, and the storativity estimated by single-well slug tests usually has questionable values (Beckie & Harvey, 2002; Bredehoeft et al., 1966; McElwee, Bohling, et al., 1995). To reduce the impact of uncertainty caused by storativity, we thus assume a spatially uniform value for the specific storage in the model.

2.2.2. Boundary and Initial Conditions
2.2.2.1. Free Water Surface Boundary in the Well
Ignoring the effect of atmospheric pressure changes, the free water surface boundary in the well can be defined as

$$T\left(\boldsymbol{v_f}, p_f\right) = 0 \quad on \ \Gamma_f, \tag{5}$$

$$u = \boldsymbol{v_f} \cdot \boldsymbol{n} \quad on \ \Gamma_f, \tag{6}$$

where u is the moving velocity of the water level. $\boldsymbol{n}$ denotes a unit vector outward and normal to the boundary of the fluid domain (Γ_f).

2.2.2.2. NS-Darcy Interfacial Boundary at the Well Screen
During slug tests, when water is exchanging at the screen interval, the near-normal flow is dominant. To describe the mass and momentum transfer at the screen, the continuity conditions of normal velocity and normal stress are adopted, where $\varnothing$ is the porosity,

$$\boldsymbol{v_f} \cdot \boldsymbol{n} = -\frac{1}{\varnothing}\boldsymbol{v_p} \cdot \boldsymbol{n} \quad on \ \Gamma_s, \tag{7}$$

$$-n^T T\left(\boldsymbol{v_f}, p_f\right)n = p_m \quad on \ \Gamma_s. \tag{8}$$

2.2.2.3. No-Flow Boundaries
The no-flow boundaries are defined as

$$(\mathbb{K}\nabla\varphi) \cdot \boldsymbol{n} = 0 \quad on \ \Gamma_{bot}, \tag{9}$$

$$(\mathbb{K}\nabla\varphi) \cdot \boldsymbol{n} = 0 \quad on \ \Gamma_{top}. \tag{10}$$

The top boundary for an unconfined aquifer can be described by specific moving water table methods. A comprehensive evaluation of this boundary is beyond the scope of this paper, and more details can be found in the work of Brindt and Wallach (2017), Jin et al. (2014), and Malama et al. (2011). In this model, the well casing is also set as no flow boundary, which means groundwater in the well and aquifer can only exchange through the well screen.

2.2.2.4. Constant-Head Boundary
For the constant-head boundary we have

$$\varphi = h_{out} \quad on \ \Gamma_{out}. \tag{11}$$

The sampling scale of the slug tests is usually smaller than that of pumping tests. Previous studies indicated that this scale is inversely proportional to the storage coefficient and can be well approximated by $r_c/\sqrt{S}$ (Beckie & Harvey, 2002; Dai et al., 2015; Karasaki et al., 1988), where r_c is the radius of well casing. Therefore, the observation well should be located within the zone of influence and the scale of the

numerical slug test model can be determined by such relationship to minimize the influence of the constant-head boundary on the simulation results.

2.2.2.5. Initial Conditions

Before the slug test is initiated, the groundwater in the well and the aquifer maintains a hydrostatic condition. Upon starting the test, the pressure equivalent to a certain height of the water column is applied rapidly on the water level boundary to induce the initial head difference. The initial conditions including the pressure, the flow rate in the well, and the head difference can be defined as follows:

$$p_f = p_m = \rho g \psi \quad at\ t = 0, \tag{12}$$

$$\boldsymbol{v_f} = 0 \quad at\ t = 0, \tag{13}$$

$$H = H_0 \quad at\ t = 0, \tag{14}$$

where ψ is the pressure head, which is measured relative to the static groundwater level. H denotes the head difference between the well and the aquifer, which means that the geometric height of the well will be reduced by H in our model.

2.3. Numerical Technique

2.3.1. The ALE Method

The ALE method is a numerical technique for solving free-surface problems (Donea et al., 2004; Duarte et al., 2004; Jin et al., 2014). By introducing referential coordinates, it redefines the node position of the calculation units which are originally defined in a spatial domain (pure Eulerian description) or material domain (pure Lagrangian description). Hence, it combines the advantages of both Lagrangian and Eulerian algorithms for the kinematic description. During a slug test, the Lagrangian method is ideal for tracking the water level fluctuation and the Eulerian method is suitable for calculating the internal pressure change. Because the motion of the free water surface boundary is mainly in to normal direction, this boundary can be assigned a Lagrangian description in the normal direction and a Eulerian description in the tangential direction. Through this method, the mesh on this boundary can adaptively move along with materials to precisely track the water level fluctuations. This fluctuation Δw is expressed as a line integration in the time domain of the flow velocity of the water in the well,

$$\Delta w = \int_0^t u\, dt. \tag{15}$$

In our 3DHIM model, after the mesh is initialized by Equations 13 and 14, the mesh deformation is forced to fit the pressure condition at the top boundary of the domain (Γ_f) which is defined by Equations 5 and 6. Finally, the updated mesh is delivered into the spatial coordinates to solve Equation 1.

2.3.2. Coordinate Transformation

Simplifying the well flow into a 2-D axisymmetric problem is reasonable in slug tests and can considerably reduce the computational cost compared to a full 3-D pipe flow model. As the coordinate systems used in the well and the aquifer are different (well: cylindrical coordinates, aquifer: Cartesian coordinates), transformation and coupling of the two coordinate systems is required. The variables on the NS-Darcy interfacial boundary (well screen boundary) can be connected by using a coordinate projection from 3-D to 2-D and transferred back by using the coordinate extrusion. These two kinds of coordinate transformation procedures can be expressed as

1. Coordinate projection: $g(r, z)|_{r\, =\, r_s} = \dfrac{\left(\int_{-\pi}^{\pi} f(X,\, Y,\, Z)\sqrt{X^2 + Y^2}\, d\theta \right)\Big|_{X^2\, +\, Y^2\, =\, r_s^2}}{2\pi\sqrt{X^2 + Y^2}},$

2. Coordinate extrusion: $f(X,\, Y,\, Z)|_{X^2\, +\, Y^2\, =\, r_s^2} = g(r,\, z)|_{r\, =\, r_s}.$

Here $\theta = atan2(y, x)$ is the arc tangent of the two variables x and y. It is similar to calculating the arc tangent of y/x, except that the signs of both arguments are used to determine the quadrant of the result, which lies in the range $[-\pi, \pi]$. r_s is the radius of the screen.

The numerical implementation of this model is realized by using the finite element software COMSOL (2012) (Cardenas & Gooseff, 2008; Hu et al., 2018; Liang et al., 2018), which is an ideal tool for coupling

variables of different physical fields. Concretely, the "Darcy's law" mode and "Free and Porous Media Flow" mode are employed to simulate groundwater movement within the aquifer and inside the well, respectively. And they are coupled by the interfacial boundary conditions. The "ALE" mode is also implemented within the wellbore domain to track the water level fluctuation.

3. Model Tests and Applications

3.1. Model Tests Considering Inertial Effects and Multilayered Aquifers

The validation procedure of the 3DHIM model is divided into two steps. First, we compare the simulation results from 3DHIM with those from analytical solutions of a homogeneous case for testing the inertial effects. Second, this 3DHIM model is tested in a multilayered heterogeneous aquifer by comparing the results from another numerical solution which does not consider inertial effects in the well.

Figure 3a shows the conceptual model of a single well slug test for a homogeneous case and the model parameters used in Butler and Zhan (2004). A partially penetrating well is embedded in a homogeneous confined aquifer with a thickness (B) of 10.64 m. The well has a radius of $r_c = 0.02$ m and a screen length of $b = 0.22$ m. The water column height from the top of the screen to the water level is 13.18 m. Two analytical solutions proposed by McElwee and Zenner (1998) and Butler and Zhan (2004) are chosen for the validation. The two analytical solutions are merely for homogeneous conditions while accounting for inertial effects in the well. Combined with the 3DHIM model, these three are all applied into a series of slug tests in a homogeneous confined aquifer (Figure 3a) with variable hydraulic conductivities, K. The simulation results are plotted in Figure 3b. It shows that the curves are very close to the analytical solution and the oscillation becomes more obvious as the value of K increases. For the multiwell slug test, we also need to assess the 3DHIM model responses at the observation well by comparison with the analytical solution of Butler and Zhan (2004). In Figure 3c, an observation well, with the same layout except the screen installed 2 m higher than the test well, is placed into the previous homogeneous aquifer. The horizontal distance between these two wells is 1 m. The simulated head responses at the observation well are shown in Figure 3d. Comparing to the analytical results for various K values shows that the 3DHIM model accurately simulates these oscillations and properly reproduces the analytical solutions. Small differences between the two types of curves can be found when K equals to 5×10^{-3} m/s, which could be due to interference of the perturbation at the observation well with the water level fluctuation in the test well. This mechanism is not included in Butler and Zhan model.

Figure 3e shows another conceptual model for validating the performance of 3DHIM in a multilayered heterogeneous aquifer. The thickness of the three-layer confined aquifer is 30 m. A 5-m-thick highly permeable layer is sandwiched in the middle, which is 15 m below the aquifer top. In this layer, a partially penetrating well is installed with a screen length of 1.25 m. A numerical model presented in Butler et al. (1994) which was developed for the case of multilevel slug tests in layered aquifers is selected. Based on the layered conceptual model (Figure 3e), a series of slug tests with different sets of hydraulic conductivities are simulated by using the 3DHIM model and the model proposed by Butler et al. (1994), assuming that the top and bottom layers have the same hydraulic conductivity. The simulated results are shown in Figure 3f, which indicates that two curves simulated by the different models are almost the same when the conductivity is low. As the K_B value of the middle layer increases, the difference between these two results first appears at early time, and then expresses in the two distinct fluctuation forms, such as overdamped or underdamped. Considering that the model of Butler et al. (1994) does not account for groundwater flow in the well, these differences are reasonable. The absence of a groundwater well means a faster response and no inertia-induced oscillations. In summary, the comparison result shows that the 3DHIM model has a good performance when simulating inertial effects in a simple heterogeneous aquifer.

3.2. Model Application to an Outcrop Analog
3.2.1. Aquifer Analog Study

To test the model performance in a highly heterogeneous formation, an outcrop analog is adopted. The outcrop analog approach is originally derived from mapping outcrops in the petroleum industry. It is also of special interest in hydrogeology due to the realistic representation of aquifer heterogeneity. It can serve as a surrogate to construct models of heterogeneous hydraulic parameter distribution. Using such analogs, with
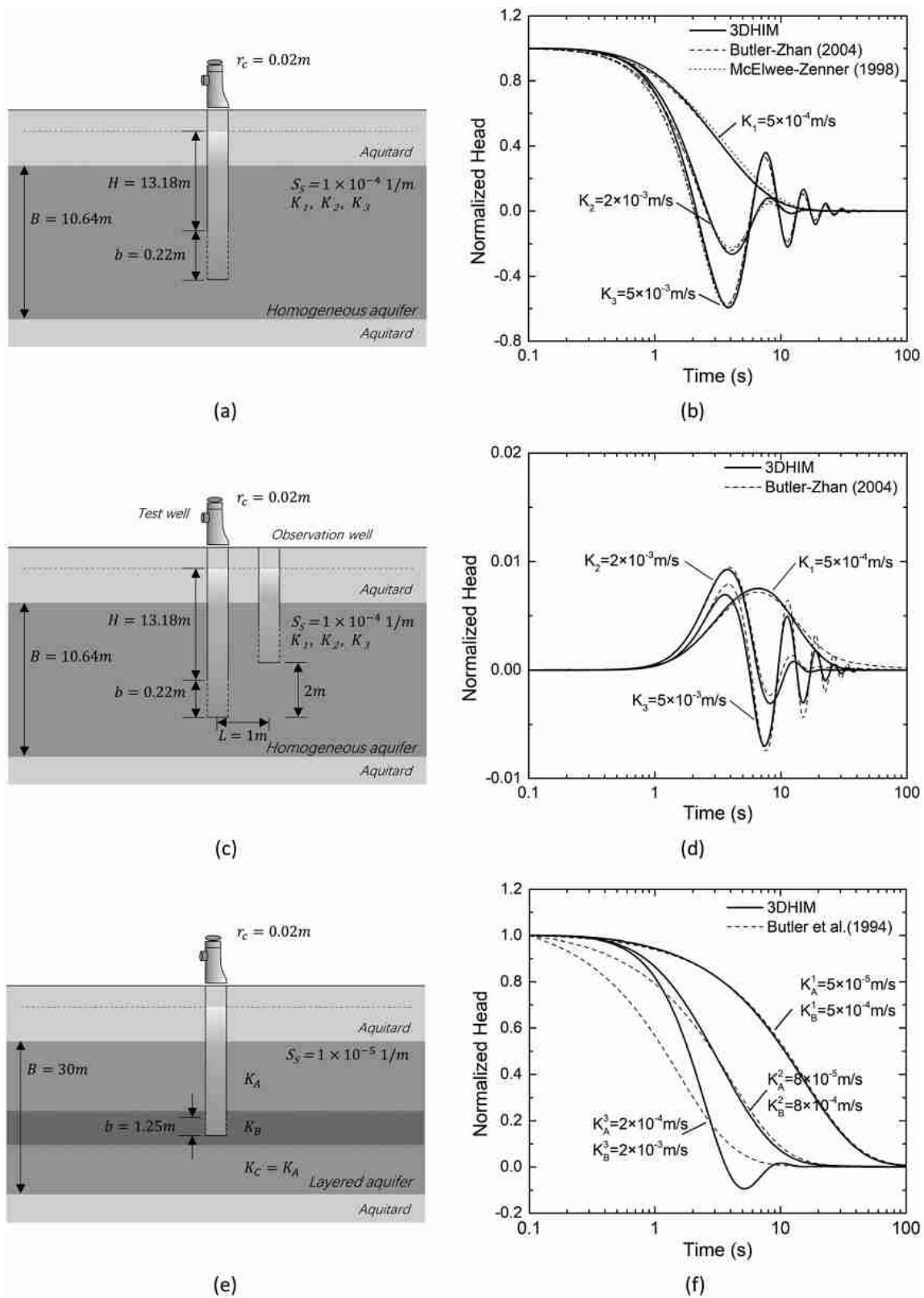
Figure 3. Validation of the 3DHIM model in a homogeneous aquifer with (a) a single well and (c) a cross-well setup, and (e) in a layered aquifer, note that the size is not to scale. The corresponding normalized head curves calculated by the analytical models (Butler & Zhan, 2004; McElwee & Zenner, 1998), a numerical model of Butler et al. (1994), and the new numerical model (3DHIM) are shown in (b), (d), and (f), respectively.
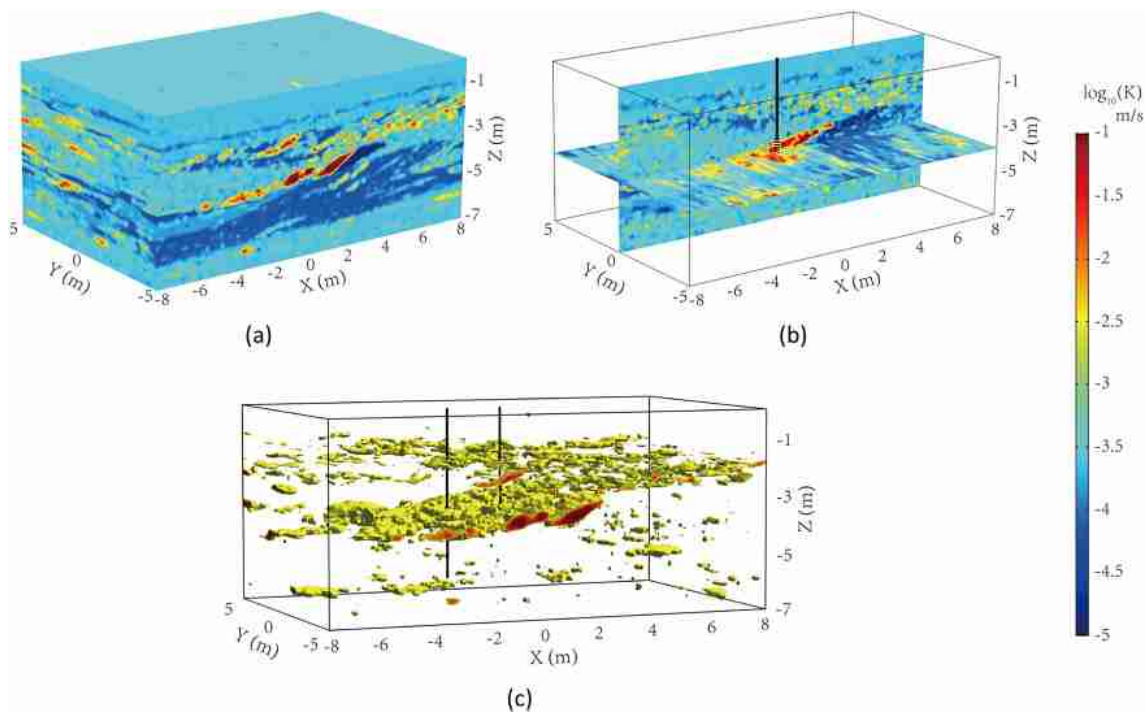
Figure 4. The reference log(K) field of the outcrop analog in (a) 3-D view, (b) cross-section view of XY-plane at z = −4 m and of *XZ*-plane at *y* = 0 m, and (c) the spatial distribution of high K zone (log(K) > −2.5). The black lines represent the wells with a screen installed at the bottom.

the fully known parameter distribution, the quality of simulated slug test result interpretation can be assessed. The 3DHIM model is applied in the following to an analog outcrop study to simulate slug tests.

The aquifer outcrop analog adopted in the following numerical investigations is developed by Bayer (2000), and it represents unconsolidated fluvial sediments near the town of Herten in southwest Germany. By digital mapping during the ongoing excavation of the sediment body in a gravel pit, vertical facies mosaics of lithology were mapped. Based on laboratory measurements of hydraulic properties, the lithology description served as basis for a hydrofacies description with dm-scale resolution of hydraulic conductivity and porosity. Maji and Sudicky (2008) further translated the gathered information into a 3-D hydraulic parameter distribution using a transition probability/Markov chain-based procedure. This outcrop analog has already been utilized in further studies, and more details can be found in Bayer et al. (2011) and Hu et al. (2011). The size of this analog is $16 \times 10 \times 7$ m, and the original numerical resolution of hydrogeological parameters is $5 \times 5 \times 5$ cm. The K value varies from 6×10^{-7} to 1 m/s. The mean value of this database is 2.11×10^{-3} m/s and its standard deviation is 0.0274 m/s. Figure 4 shows the $\log_{10}$-hydraulic conductivity field in 3-D and cross-section views, and the spatial distribution of a relatively high K zone in which K is above ca. 3×10^{-3} m/s ($\log_{10}(K) > -2.5$).

3.2.2. Single-Well Slug Tests With Various Well Geometries

The single-well slug test is the most common way to obtain the local hydraulic parameters near the well. Combined with multiple packer systems, depth oriented single-well multilevel slug tests can be used to resolve the vertical change of hydraulic conductivity around the well. In a homogeneous model, due to the inertial effects, the water level response in the well is not only affected by the aquifer hydraulic conductivity, but also by the well geometry, including the pipe radius r, screen length b and water column height H. A smaller well radius, a longer screen length, or a larger water column height can result in a more significant water level oscillation in a highly permeable aquifer. Therefore, interpretation of the water level response of the test well in a heterogeneous aquifer should also consider the impact of well geometries. To investigate these factors, based on the outcrop analog, a series of single-well slug tests with different well radii, water column heights, and screen lengths are simulated. The test well is located at the center of the analog, and three levels are selected for each well parameter (r: 0.01, 0.03, 0.05 m; b:0.1, 0.2, 0.5 m; H:1.8, 3.8, 5.8 m).
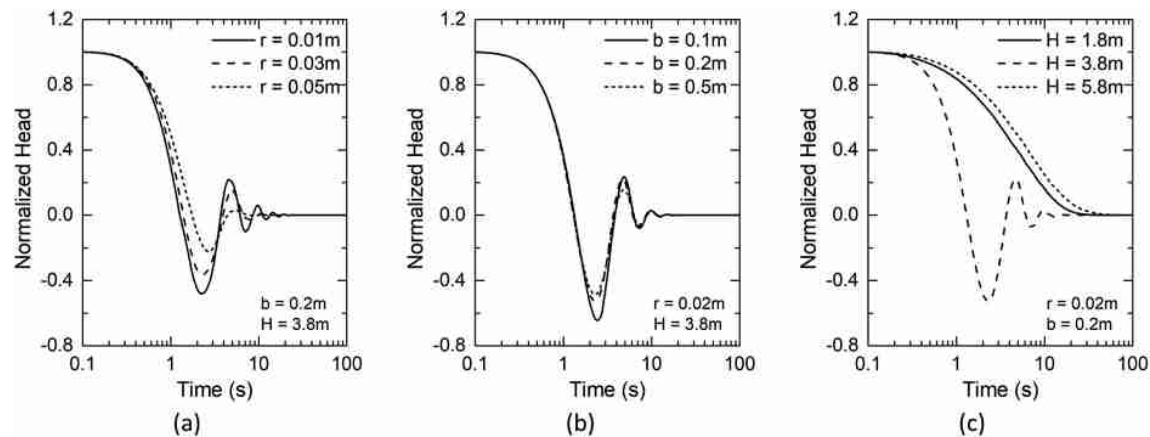
Figure 5. The curves of the normalized head in single-well slug tests with various (a) well radii, (b) screen lengths, and (c) water column heights.

Figure 5 shows the curves of the normalized head in the test wells with various well radii, screen lengths, and water column heights. The results in Figure 5a indicate that the water level oscillation is intensified as the well radius decreases. This trend is consistent with that in the homogeneous aquifers. However, as shown in Figures 5b and 5c, the oscillation of the curves is no longer intensified as the screen length and water column height increases, which is distinct from the homogeneous cases. This is because the results from the various screen lengths and water column heights are heavily affected by the heterogeneous conductivity distribution. When $b = 0.1$ m or $H = 3.8$ m, the water level curve has the largest oscillation amplitude, because there is a thin and highly permeable layer near the depth of -4.0 m at the well location (Figure 4c). When the screen length or water column height is changed, the position of the screened interval is also changed. These simulation results indicate that the water level response in the test well shows the combined effect of well geometry and heterogeneous conductivity.

3.2.3. Cross-Well Slug Tests Considering Inertial and Skin Effects

The cross-well slug test is another way to obtain hydraulic parameters, which can vastly improve parameter estimation in space (McElwee, Butler, et al., 1995). Specifically, a cross-well tomographic slug test can provide spatial heterogeneity of hydraulic parameters. In addition to the influence of well geometry, the oscillating water level is also affected by the inertia of the water column, which is often ignored in heterogeneous models, and by skin effects. In order to investigate the influence of in-well inertial and skin effects around the wells in heterogeneous aquifers on test results, based on the Herten analog, four numerical cases of cross-well slug tests are designed:

Case 1: a test well and three observation points with the depths of 2, 4, and 6 m, respectively;
Case 2: a test well and a 2-m deep observation well;
Case 3: a test well and a 4-m deep observation well;
Case 4: a test well and a 6-m deep observation well.

In fact, *Case 1* can serve as a control case to compare pressure changes with or without observation wells. The other three cases are used to compare water level changes in observation wells at different depths considering inertial and skin effects. First, to facilitate a comparison of the results impacted by the inertial effects between different cases and to distinguish the pressure diffusion process in aquifers and wells, three types of head changes at observation points, midpoints of the screen, and water levels in the wells are monitored. Subsequently, a certain thickness of skin is added around both wells in each case. The water levels in each well are also recorded.

The settings of all cases are shown in Figure 6. The bottom of the test well is 4 m below the aquifer top. The radius of the riser pipe and screen are 0.017 and 0.03 m, respectively. The screen length is 0.2 m. The horizontal distance between the test well and observation points or wells is 2 m. As mentioned in section 2.2, the specific storage is defined as a spatially uniform value, which is set here 1×10^{-4} m^{-1}. We assume an initial head of zero everywhere in the aquifer with an initial displacement of the water level in the test well by 1 m.
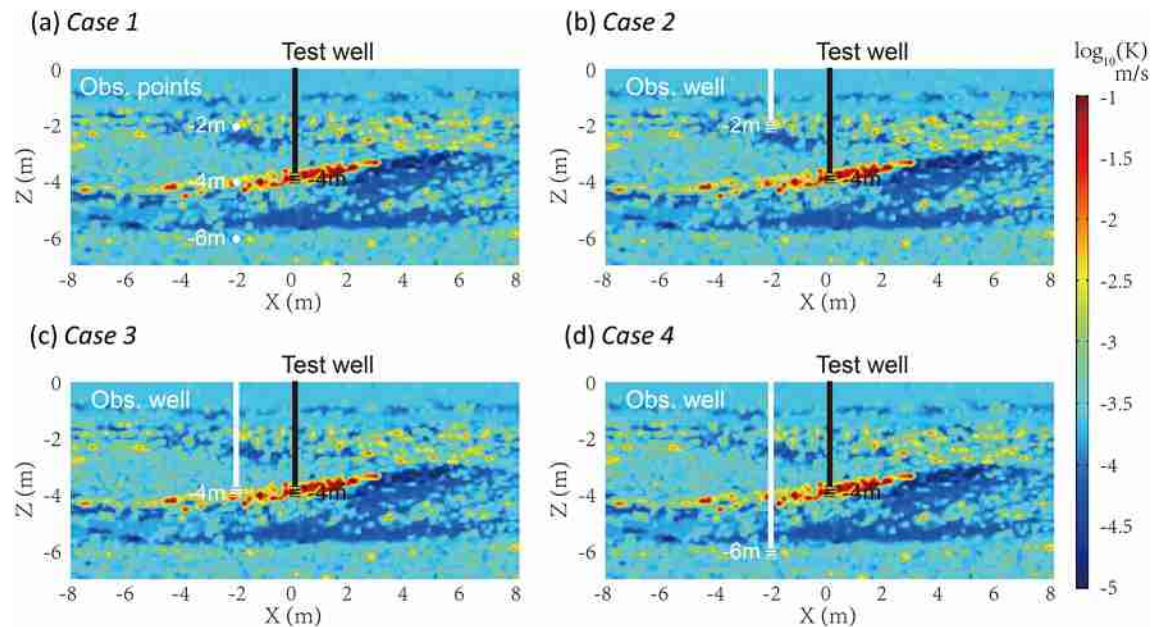
Figure 6. (a) Case 1, (b) Case 2, (c) Case 3, (d) Case 4, the settings of the four cases of cross-well slug tests in the view of the *XZ*-plane at *Y* = 0.
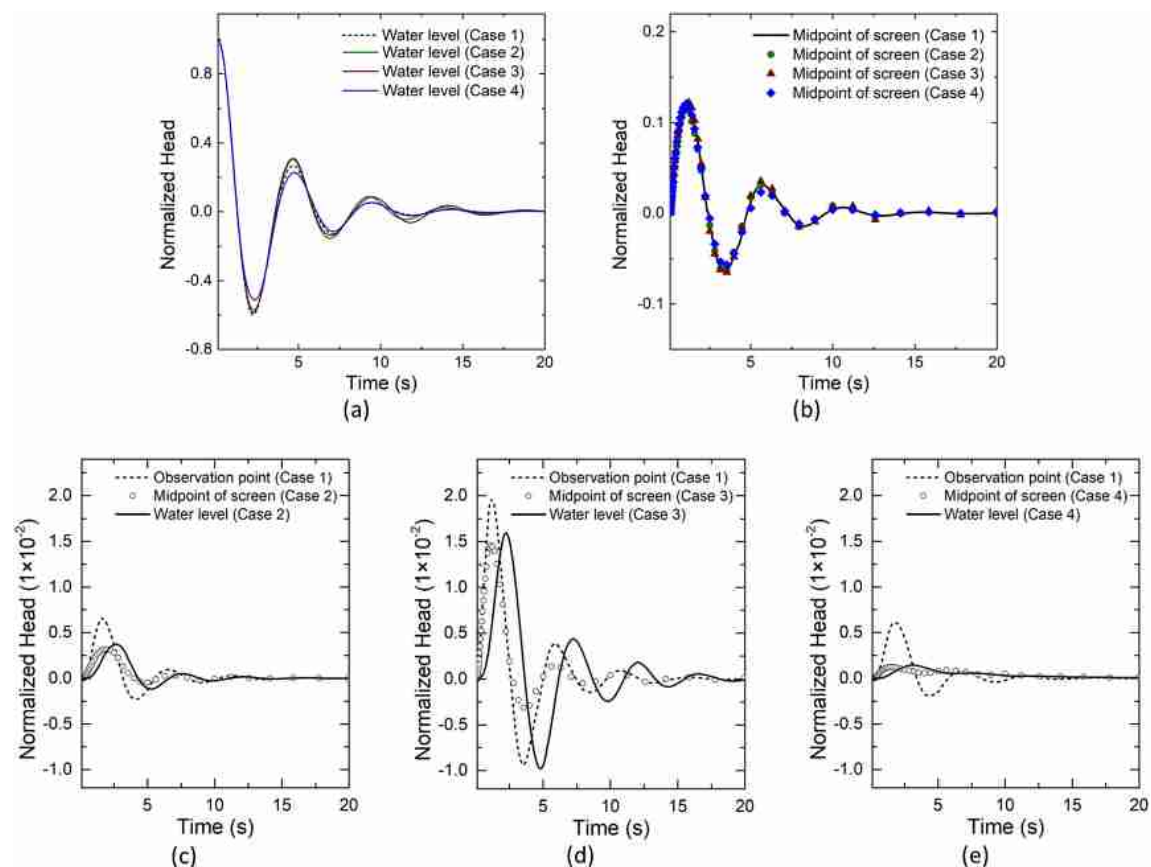

Figure 7. Normalized curves of (a) water level and (b) head at the midpoint of the screen in the test well, and the normalized head responses from the observation point, midpoint of the screen and the water level at the various observation wells/point depths of (c) 2 m, (d) 4 m, and (e) 6 m.

The impact of inertial effects to the water level in the wells without skin effects is firstly assessed. The simulation results are depicted in Figure 7. Four test-well normalized head curves are initially obtained (Figure 7a). As shown, the phases of these oscillatory curves are virtually identical, while the amplitudes are slightly different. Considering the curve of *Case 1* as a reference, the curve amplitudes from *Case 2* and *Case 3* are increased especially at the first peak. In comparison, the head amplitude from *Case 4* is always smaller. This result shows that the embedded observation wells have slightly interfered with the water level fluctuations in the test well. According to the superposition principle, the perturbation at the observation well can in turn influence the water level at the test well, especially when two wells are positioned at a short distance. This amplifies or damps the water level oscillations in the test well, depending on the embedded well depth and the hydraulic connectivity contrast between the test and observation wells. The head curve at the midpoint of the screen is utilized to replace the pressure change in the aquifer close by the test interval. The head curves at the midpoints of the screen in the four test wells are depicted in Figure 7b. All head curves have a large attenuation and phase shift compared to the water levels, and the differences between these curves are reduced.

The head change curves from observation points or wells are plotted in Figures 7c–7e, which includes three head curves of the observation points from *Case 1*, three water level curves and three head curves at the midpoint of each screen in the observation wells from *Case 2*, *Case 3*, and *Case 4*, respectively. First, we compare the heads from the observation points (dashed lines) and the midpoint of the screen (circles) at the same depth to reveal the pressure changes in the aquifer before and after the installation of the observation well. It can be found, especially in Figure 7e, that the head of the midpoints of screen is significantly reduced. This reveals that the installation of the observation well reduced the normalized head amplitude near the observation interval.

Second, comparing the water level curves (solid lines) with the head curves at the midpoints of screen (circles), the influence of inertial effects in the well on water level fluctuations can be evaluated. The results show that the water level curves present obvious phase delay and amplitude change. Especially in Figure 7d, the amplitude of the oscillatory water level is significantly enhanced after the first peak. It implies that the inertial effect in the well can enhance the amplitude of the water level. However, in Figures 7c and 7e, the enhancement of the amplitude is not obvious, which indicates that this amplification may depend on the depth of the well and the aquifer heterogeneity.

Considering the important role of skin effects in multiwell slug testing, their impact on the water level responses in test and observation wells is evaluated. Generally, the hydraulic conductivity of the skin can either be higher or lower than that of the ambient formation. Based on the outcrop analog, a low-K and a high-K value, which are 0.1 times and 5 times of the original K, are therefore assigned to the simulated skin around the wells. To eliminate the effect of the skin thickness on the simulated results, the infinitely thin skin model which has been used in well hydraulics field for decades (Dougherty & Babu, 1984; Faust & Mercer, 1984; Ramey et al., 1975) is adopted. The groundwater flow in the skin region is accounted for by the steady-state representation of the groundwater flow equation, which neglects elastic storage properties. Therefore, head changes caused by the different types of skin are only related to the ratio of the K value of the skin to that of the original formation. The impact of the skin effects can be demonstrated directly by comparing the head responses under various skin K-values. Based on the Cases 2, 3, and 4 shown in Figure 6, two additional series of cross-well slug tests with low-K skin and high-K skin are simulated. The results including the water level responses with no skin effect (shown in Figure 7) are both plotted in the Figure 8. The result reveals that the low-K skin has a much larger effect on the water level responses in the wells than high-K skin. The effect of the high-K skin is quite small, while the low-K skin significantly dampens the oscillatory behavior of the water level, especially in the observation well. These results are consistent with the findings in many previous studies (Butler et al., 1994; Hyder et al., 1994; Malama et al., 2011).

4. Discussion

4.1. Wellbore Storage Effects of Observation Wells Controlled by Aquifer Heterogeneity

As shown in Figures 7c–7e, after observation wells are installed, the pressure around the observation interval represented by the head at the midpoint of the screen is obviously attenuated. In fact, groundwater wells are often considered to be conduits for fast groundwater flow and contaminant migration (Chesnaux et al., 2006;
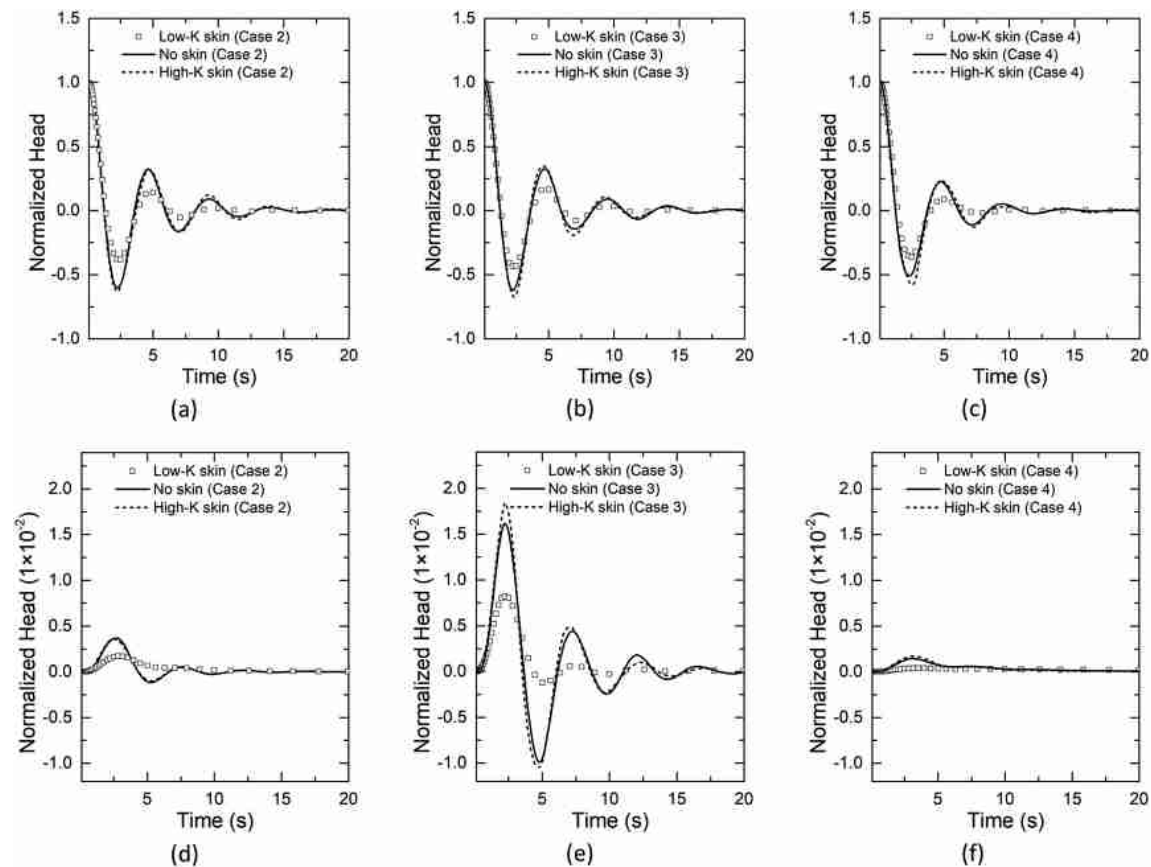
Figure 8. Normalized curves of water level in cross-well slug tests with low-K skin, no skin, and high-K skin. The curves in (a)–(c) and (d)–(f) show the head responses at the test well and at the observation well in Cases 2, 3, and 4, respectively.

Koh et al., 2016; Lacombe et al., 1995). This means observation wells have the capacity to release the pressure rapidly from the aquifer, i.e., they may show wellbore storage effects. However, due to aquifer heterogeneity, the wellbore storage effects of the observation wells embedded at different depths are variable. For the observation depth of 4 m, the head amplitude in the aquifer is reduced only slightly before and after the observation well is installed, due to the highly permeable layer at about 4 m depth. In contrast, being embedded in a low conductivity zone, the head amplitude at the bottom of the 6-m observation well is strongly attenuated. If the observation well is considered as a fast flow conduit, the head amplitude at the midpoint of the screen directly reflects the conductivity near the observation interval. Accordingly, the wellbore storage effects of the observation well depends heavily on the conductivity distribution close to the observation interval. The higher the conductivity is, the stronger the wellbore storage effects could be.

To more clearly illustrate the relationship between the wellbore storage effects and aquifer heterogeneity, the XZ-plane profiles of the four cases at $Y = 0$ are chosen. Their normalized head contour maps at 2.3 s are shown in Figure 9. At this moment, the water levels in all test wells almost reach the minimum value and the heads at the bottom of these wells are around zero (see Figures 7a and 7b). Here the minimum value of the normalized head in the legend is adjusted to -0.01 to have the aquifer pressure gradient more clearly displayed. Figure 9 illustrates that the contour line at the bottom of each observation well has shrunk inward. Especially in Figure 9d, due to the low conductivity, the contour line is concave at the bottom of the observation well. Moreover, comparing to Figure 9a, the influence range of the test wells in the other three maps is reduced, particularly in Figures 9b and 9d. In Figure 9c, this impact of reduction is relatively weak, because there is a good hydraulic connection between the observation and the test well. All these results indicate that the wellbore storage mechanism of the observation well will introduce a pressure redistribution according to the hydraulic conductivity in the vicinity of the observation interval.
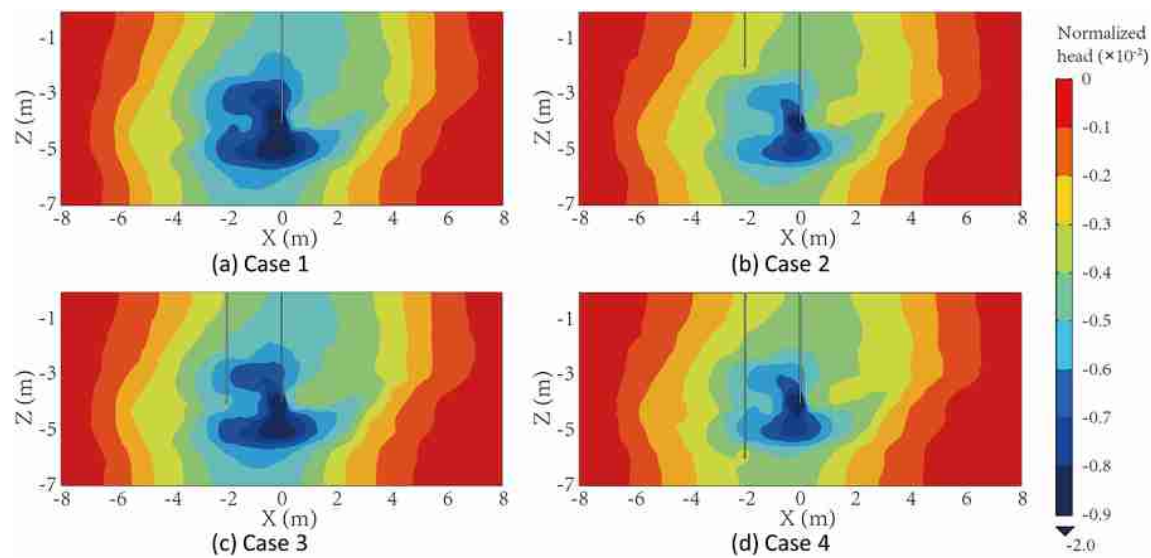
Figure 9. (a) Case 1, (b) Case 2, (c) Case 3, (d) Case 4, normalized head contour map on the *XZ*-plane profiles (at *Y* = 0 m) of the four cases at 2.3 s after slug test initiated.

For the test well, the difference of the hydraulic dissipation process in the four cases can also be attributed to wellbore storage effects. It has been discussed in numerous single-well slug test studies (Bredehoeft et al., 1966; Hyder et al., 1994; McElwee & Zenner, 1998) that the wellbore storage capacity recorded by the water level fluctuation is dominated by the aquifer hydraulic conductivity. However, in cross-well slug tests, the impact of wellbore storage effects will be more complicated, due to a pressure redistribution within the heterogeneous test volume and in turn an impact on the water level recovery in the test well (Figure 7a).

4.2. Inertial Effect of the Water Column in Cross-Well Slug Tests

Another important factor influencing the cross-well slug test results is inertia of the water column moving inside the well. The inertial effect manifests as oscillatory well water level response. Butler and Zhan (2004) considered inertial effects by using the simplified momentum balance equation in their homogeneous slug test model and pointed out that inertial mechanisms can have a dramatic impact on the early-time drawdown. However, so far these inertial effects are rarely considered in heterogeneous models.

In the presented analog outcrop study, the water level oscillations induced by inertial effects are obvious. When compared with the head curves at the midpoint of the screen in each observation well in Figures 7c–7e, it is revealed that the water level curves not only show a phase shift but also an amplitude enhancement. To quantify the differences between these two types of curves, the maximum amplitude and its corresponding peak time are calculated and plotted in Figure 10. In Figure 10a, the peak times of these two types of curves are significantly different. The peak time of the water level is always larger. Aside from this, the difference line (dashed line) reveals a near-linear correlation between the peak time difference and the observation depth, i.e., the water column height. From the perspective of maximum amplitude, we can see that the values of the water level are slightly higher, especially for the 4-m observation depth.

Consideration of the hydrodynamic process in the well will inevitably lead to a peak-time delay of the water level compared to the head curve at the well bottom, and this delay should be proportional to the water column height in this well. In addition, the inertial effects can also enhance the water-level amplitude. Cooper et al. (1965) discussed this amplification effect of the well, which is used to describe the water level response to harmonic seismic waves. If the head excited in the test well is viewed as an attenuating wave source, the amplification theory can be equally applied to interpret water level response of the observation well in the cross-well slug tests. When the test is initiated, the observation well will show a response according to its "natural frequency," which is determined by the well geometry and aquifer transmissivity. When the observation well and test well have a good hydraulic connection and follow a similar natural frequency, a
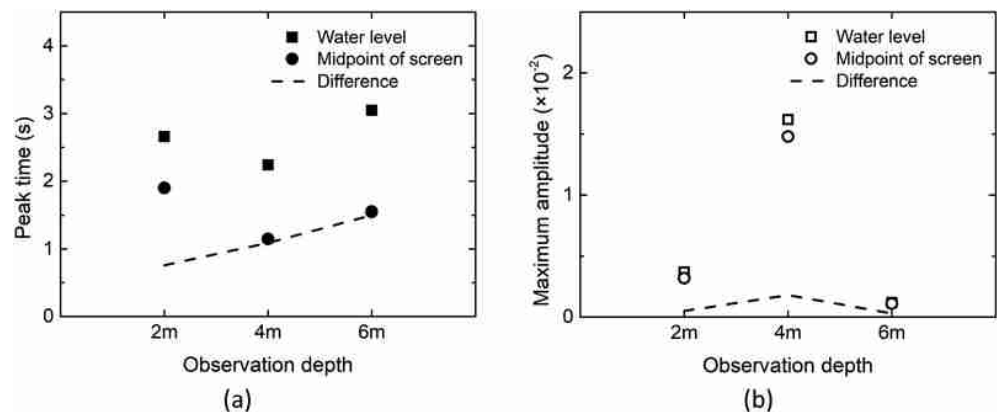
Figure 10. The peak time (a) and maximum amplitude (b) of the water level and head curves at midpoint of the screen at different depths of observation wells. The corresponding differences between water level and head at the midpoint of the screen are given by the dashed line.

water-level resonance may even occur. For example, in *Case 3*, the water-level amplitudes are significantly amplified, especially after the first peak (Figure 7d). Together with the water level curve in the test well, a resonance behavior can be inferred in this case. However, the impact of the amplification effect will generally be diminished in space, because the hydraulic disturbance in the slug test is weak and will be further attenuated by the heterogeneous aquifer. In short, considering the well effects, such as inertial and wellbore storage effects, will result in a phase and amplitude change in the water level curves. Indeed, despite the amplification of the water level amplitude exists, it can take place only under special conditions, such as a very good hydraulic connection but a small distance between the test interval and the observation interval.

4.3. Potential Error Analysis Without Well Effects

One of the main purposes of slug test modeling is to estimate aquifer parameters. Based on the corresponding relations established by the mathematical model, the heterogeneous parameters could be inverted through the water level response by using some inversion algorithms (Brauchler et al., 2007, 2010, 2011; Yang et al., 2015; Zhu & Yeh, 2005). However, the water level response not only represents the hydraulic signal propagation process within the aquifer but also the well effects. If these effects are not considered, the hydraulic parameters estimated directly from the water level will therefore include potential errors.

In early studies using heterogeneous models (Butler et al., 1994; Melville et al., 1991; Widdowson et al., 1990), groundwater flow in the well is neglected. Without well effects, these models cannot handle the oscillatory water level response, and the simulated head will not attenuate following the wellbore storage mechanism. This resulting estimation error can only be diminished in low conductivity aquifers with a large well spacing. Subsequently, although the groundwater flow in the well has been considered in some models, it is replaced by the Darcian flow with a high conductivity value (Brauchler et al., 2007; Yang et al., 2015). This means that it is still difficult to handle the oscillatory water level by these improved models, because the inertial term is ignored. However, the wellbore storage effects of the well are somewhat included. To date, the suitability of these models in highly permeable aquifers remains to be examined. Although the inertia-induced oscillation of the water level in observation well could be neglected when the distance from the test well is sufficiently large, McElwee, Butler, et al. (1995) pointed out that only an observation well fairly close to the test well, at a distance of about 10 m or less, can vastly improve parameter estimates, and it is suggested to use one or more observation wells. In order to improve the parameter estimation, a closer well spacing would be required. Moreover, previous work (Quinn et al., 2018; Zurbuchen et al., 2002) has shown that frictional losses within the well casing and screen play an important role in testing highly conductive media. Ignoring friction losses will lead to an underestimated hydraulic conductivity. This means that a more rigorous slug test model is needed, which can consider well effects, aquifer heterogeneity, and head losses within the casing and at the screen.

5. Conclusions

In this work, 3DHIM, a 3-D slug test model considering inertial effects both in test and observation wells in a heterogeneous aquifer is introduced. After inspecting various existing models of slug test analysis, two analytical solutions (Butler & Zhan, 2004; McElwee & Zenner, 1998) and a numerical solution of Butler et al. (1994) are chosen to compare the slug test results obtained using the new 3DHIM model. Based on a successful validation, this model is finally used to simulate a series of synthetic slug tests in a highly heterogeneous 3-D aquifer outcrop analog, which has been developed during the excavation of unconsolidated glacio-fluvial sediments near the town of Herten in southwest Germany.

Single-well slug tests with varying well radius, water column height, and screen length are firstly simulated within the synthetic heterogeneous aquifer. Unlike in a homogeneous aquifer, the results show that the water level oscillations in the test well are no longer sensitive to the screen length and water column height, but are heavily affected by inertial effects of the water column and by heterogeneity of hydraulic conductivity at the well test interval.

Based on the established single-well slug test model, three observation wells with different depths (i.e., 2, 4, and 6 m) are installed 2 m away from the test well. Together with the single-well slug test (without observation well), the water levels and pressure changes in the aquifer in these four cases are compared to study the impact of inertial effects. Results show that the water level fluctuations do not only reflect the hydraulic signal propagation process within the aquifer but also wellbore storage and water column inertial effects. Specifically, wellbore storage effects at the observation well yield a pressure redistribution within the aquifer and a large water level amplitude change, which is related to the heterogeneity of hydraulic conductivity near the observation interval. The water column inertia in both test and observation wells will result in a phase shift of the water level fluctuation, which is proportional to the water column height. When the observation well and the test well have a good hydraulic connection and similar well geometry, the water level amplitude could be amplified. Therefore, if these effects are not considered, the hydraulic parameter estimation based on water level will potentially be incorrect.

Although the new 3DHIM model allows to consider water column inertial effects in heterogeneous aquifers, it still has some challenges. It assumes a linear friction force within the riser pipe and screen, and it ignores non-Darcian flow within the skin or aquifer. The influence of water column inertia on the parameter estimation in heterogeneous aquifer remains to be studied. In any case, the proposed model provides a reliable tool to explain the oscillatory water level response in a 3-D heterogeneous aquifer.

Appendix A: The Derivation of Equation 1 and its Weak Form

Within the wellbore region (Ω_f), we assume that the groundwater motion can be described by the incompressible NS equation as Equation 1. This particular form is derived from the generic Cauchy momentum equation (Goraj, 2016)

$$\rho \frac{D\boldsymbol{v_f}}{Dt} = \nabla \cdot T + f, \tag{A1}$$

where $\frac{D}{Dt}$ is the material derivative, defined as $\frac{\partial}{\partial t} + \boldsymbol{v_f} \cdot \nabla$; T is the Cauchy stress tensor; and f represents the body forces. Within the incompressible fluid domain, the Cauchy stress tensor can be set to the sum of a pressure term $-p_f \boldsymbol{I}$ and a viscosity term $\mu(\nabla \boldsymbol{v_f} + (\nabla \boldsymbol{v_f})^T)$.

During the slug test, the groundwater flow in the well is dominated by the vector of flow velocity $\boldsymbol{v_f}(\boldsymbol{u}, \boldsymbol{v}, \boldsymbol{w})$ and scalar pressure p. In 3-D cartesian coordinates, the symmetric stress tensor can be written as (Malvern, 1969)

$$T = \begin{bmatrix} -p + 2\mu\dfrac{\partial \boldsymbol{u}}{\partial x} & \mu\left(\dfrac{\partial \boldsymbol{u}}{\partial y} + \dfrac{\partial \boldsymbol{v}}{\partial x}\right) & \mu\left(\dfrac{\partial \boldsymbol{u}}{\partial z} + \dfrac{\partial \boldsymbol{w}}{\partial x}\right) \\[2ex] & -p + 2\mu\dfrac{\partial \boldsymbol{v}}{\partial y} & \mu\left(\dfrac{\partial \boldsymbol{v}}{\partial z} + \dfrac{\partial \boldsymbol{w}}{\partial y}\right) \\[2ex] & & -p + 2\mu\dfrac{\partial \boldsymbol{w}}{\partial z} \end{bmatrix}. \tag{A2}$$

To improve computing efficiency, the groundwater flow in the well can be simplified to axisymmetric flow. Equation A1 can be transformed from cartesian coordinates (x, y, z) to cylindrical coordinates (r, θ, z) by using an operator,

$$\Lambda = \frac{\partial}{\partial r} r + \frac{1}{r} \frac{\partial}{\partial \theta} \theta + \frac{\partial}{\partial z} z. \tag{A3}$$

For the axisymmetric flow, the tensor can be expressed as (Malvern, 1969)

$$T = \begin{bmatrix} -p + 2\mu \frac{\partial \boldsymbol{u}}{\partial r} & \mu \left[r \frac{\partial}{\partial r} \left(\frac{\boldsymbol{v}}{r} \right) + \frac{1}{r} \frac{\partial \boldsymbol{u}}{\partial \theta} \right] & \mu \left(\frac{\partial \boldsymbol{u}}{\partial z} + \frac{\partial \boldsymbol{w}}{\partial r} \right) \\ & -p + 2\mu \left(\frac{1}{r} \frac{\partial \boldsymbol{v}}{\partial \theta} + \frac{\boldsymbol{u}}{r} \right) & \mu \left(\frac{\partial \boldsymbol{v}}{\partial z} + \frac{1}{r} \frac{\partial \boldsymbol{w}}{\partial \theta} \right) \\ & & -p + 2\mu \frac{\partial \boldsymbol{w}}{\partial z} \end{bmatrix}. \tag{A4}$$

In order to find the variational form for numerical analysis, the weak form of Equation A1 can be expressed as

$$0 = -\int_{\Omega_f} \rho \left[\frac{\partial \boldsymbol{v_f}}{\partial t} + (\boldsymbol{v_f} \cdot \nabla) \boldsymbol{v_f} \right] \cdot \boldsymbol{\tau} - \int_{\Omega_f} T \cdot \nabla \boldsymbol{\tau} + \int_{\Omega_f} f \cdot \boldsymbol{\tau} + \int_{\Gamma_f} T \cdot \boldsymbol{\tau}. \tag{A5}$$

Accordingly, this weak form can be solved by the finite element method, such as implemented in the COMSOL software, and coupled with Darcy's law for description of groundwater flow (Hanspal et al., 2006).

Data Availability Statement

Related data sets are available online (http://doi.org/10.5281/zenodo.3946490).

References

Alazmi, B., & Vafai, K. (2001). Analysis of fluid flow and heat transfer interfacial conditions between a porous medium and a fluid layer. *International Journal of Heat and Mass Transfer*, *44*(9), 1735–1749. https://doi.org/10.1016/S0017-9310(00)00217-9

Bayer, P. (2000). *Aquifer-Analog-Studie in grobklastischen 'braided river'Ablagerungen: Sedimentäre/hydrogeologische Wandkartierung und Kalibrierung von Georadarmessungen—Diplomkartierung*. Diplomkartierung: Universitaet Tuebingen.

Bayer, P., Huggenberger, P., Renard, P., & Comunian, A. (2011). Three-dimensional high resolution fluvio-glacial aquifer analog: Part 1: Field study. *Journal of Hydrology*, *405*(1–2), 1–9. https://doi.org/10.1016/j.jhydrol.2011.03.038

Beckie, R., & Harvey, C. F. (2002). What does a slug test measure: An investigation of instrument response and the effects of heterogeneity. *Water Resources Research*, *38*(12), 1290. https://doi.org/10.1029/2001WR001072

Braester, C., & Thunvik, R. (1984). Determination of formation permeability by double-packer tests. *Journal of Hydrology*, *72*(3–4), 375–389. https://doi.org/10.1016/0022-1694(84)90090-8

Brauchler, R., Cheng, J.-T., Dietrich, P., Everett, M., Johnson, B., Liedl, R., & Sauter, M. (2007). An inversion strategy for hydraulic tomography: Coupling travel time and amplitude inversion. *Journal of Hydrology*, *345*(3–4), 184–198. https://doi.org/10.1016/j.jhydrol.2007.08.011

Brauchler, R., Hu, R., Dietrich, P., & Sauter, M. (2011). A field assessment of high-resolution aquifer characterization based on hydraulic travel time and hydraulic attenuation tomography. *Water Resources Research*, *47*, W03503. https://doi.org/10.1029/2010WR009635

Brauchler, R., Hu, R., Vogt, T., Al-Halbouni, D., Heinrichs, T., Ptak, T., & Sauter, M. (2010). Cross-well slug interference tests: An effective characterization method for resolving aquifer heterogeneity. *Journal of Hydrology*, *384*(1–2), 33–45. https://doi.org/10.1016/j.jhydrol.2010.01.004

Bredehoeft, J. D., Cooper, H. H. Jr., & Papadopulos, I. S. (1966). Inertial and storage effects in well-aquifer systems: An analog investigation. *Water Resources Research*, *2*(4), 697–707. https://doi.org/10.1029/WR002i004p00697

Brindt, N., & Wallach, R. (2017). The moving-boundary approach for modeling gravity-driven stable and unstable flow in soils. *Water Resources Research*, *53*, 344–360. https://doi.org/10.1002/2016WR019252

Butler, J. J. Jr. (2002). A simple correction for slug tests in small-diameter wells. *Ground Water*, *40*(3), 303–308. https://doi.org/10.1111/j.1745-6584.2002.tb02658.x

Butler, J. J., Bohling, G. C., Hyder, Z., & Mcelwee, C. D. (1994). The use of slug tests to describe vertical variations in hydraulic conductivity. *Journal of Hydrology*, *156*(1–4), 137–162. https://doi.org/10.1016/0022-1694(94)90075-2

Butler, J. J., & Zhan, X. Y. (2004). Hydraulic tests in highly permeable aquifers. *Water Resources Research*, *40*, W12402. https://doi.org/10.1029/2003WR002998

Cardenas, M. B., & Gooseff, M. N. (2008). Comparison of hyporheic exchange under covered and uncovered channels based on linked surface and groundwater flow simulations. *Water Resources Research*, *44*, W03418. https://doi.org/10.1029/2007WR006506

Cardiff, M., Barrash, W., Thoma, M., & Malama, B. (2011). Information content of slug tests for estimating hydraulic properties in realistic, high-conductivity aquifer scenarios. *Journal of Hydrology*, *403*(1–2), 66–82. https://doi.org/10.1016/j.jhydrol.2011.03.044

Chesnaux, R., Chapuis, R., & Molson, J. (2006). A new method to characterize hydraulic short-circuits in defective borehole seals. *Groundwater*, *44*(5), 676–681.

Cimolin, F., & Discacciati, M. (2013). Navier–Stokes/Forchheimer models for filtration through porous media. *Applied Numerical Mathematics*, *72*, 205–224. https://doi.org/10.1016/j.apnum.2013.07.001

Clemo, T. (2010). Coupled aquifer-borehole simulation. *Groundwater*, *48*(1), 68–78. https://doi.org/10.1111/j.1745-6584.2009.00597.x

Cooper, H. H. Jr., Bredehoeft, J. D., Papadopulos, I. S., & Bennett, R. R. (1965). The response of well-aquifer systems to seismic waves. *Journal of Geophysical Research*, *70*(16), 3915–3926. https://doi.org/10.1029/JZ070i016p03915

Dai, Y., Zhou, Z., Zhao, Y., & Cui, Z. (2015). Evaluation of the effects of the radial constant-head boundary in slug tests. *Hydrogeology Journal*, *23*(4), 807–818. https://doi.org/10.1007/s10040-015-1240-7

Donea, J., Huerta, A., Ponthot, J.-P., & Rodriguez-Ferran, A. (2004). *Arbitrary Lagrangian-Eulerian Methods, volume 1 of Encyclopedia of Computational Mechanics, chapter 14* (Vol. 3, pp. 1–25). New Jersey, USA: John Wiley & Sons Ltd. https://doi.org/10.1002/0470091355.ecm009

Dougherty, D., & Babu, D. (1984). Flow to a partially penetrating well in a double-porosity reservoir. *Water Resources Research*, *20*(8), 1116–1122. https://doi.org/10.1029/WR020i008p01116

Duarte, F., Gormaz, R., & Natesan, S. (2004). Arbitrary Lagrangian–Eulerian method for Navier–Stokes equations with moving boundaries. *Computer Methods in Applied Mechanics and Engineering*, *193*(45–47), 4819–4836. https://doi.org/10.1016/j.cma.2004.05.003

Faust, C. R., & Mercer, J. W. (1984). Evaluation of slug tests in wells containing a finite-thickness skin. *Water Resources Research*, *20*(4), 504–506. https://doi.org/10.1029/WR020i004p00504

Goraj, R. (2016). Transformation of the Navier-Stokes equation to the Cauchy Momentum equation using a novel mathematical notation. *Applied Mathematics*, *07*(10), 1068–1073. https://doi.org/10.4236/am.2016.710094

Hanspal, N. S., Waghode, A. N., Nassehi, V., & Wakeman, R. J. (2006). Numerical analysis of coupled Stokes/Darcy flows in industrial filtrations. *Transport in Porous Media*, *64*(1), 73–101. https://doi.org/10.1007/s11242-005-1457-3

Hanspal, N. S., Waghode, A. N., Nassehi, V., & Wakeman, R. J. (2009). Development of a predictive mathematical model for coupled stokes/Darcy flows in cross-flow membrane filtration. *Chemical Engineering Journal*, *149*(1–3), 132–142. https://doi.org/10.1016/j.cej.2008.10.012

Houben, G. J. (2015). Hydraulics of water wells—Flow laws and influence of geometry. *Hydrogeology Journal*, *23*(8), 1633–1657. https://doi.org/10.1007/s10040-015-1312-8

Hu, R., Brauchler, R., Herold, M., & Bayer, P. (2011). Hydraulic tomography analog outcrop study: Combining travel time and steady shape inversion. *Journal of Hydrology*, *409*(1–2), 350–362. https://doi.org/10.1016/j.jhydrol.2011.08.031

Hu, R., Liu, Q., & Xing, Y. (2018). Case study of heat transfer during artificial ground freezing with groundwater flow. *Water*, *10*(10), 1322. https://doi.org/10.3390/w10101322

Hyder, Z., Butler, J. J. Jr., McElwee, C. D., & Liu, W. (1994). Slug tests in partially penetrating wells. *Water Resources Research*, *30*(11), 2945–2957. https://doi.org/10.1029/94WR01670

Jin, Y., Holzbecher, E., & Sauter, M. (2014). A novel modeling approach using arbitrary Lagrangian–Eulerian (ALE) method for the flow simulation in unconfined aquifers. *Computers & Geosciences*, *62*, 88–94. https://doi.org/10.1016/j.cageo.2013.10.002

Kabala, Z., Pinder, G., & Milly, P. (1985). Analysis of well-aquifer response to a slug test. *Water Resources Research*, *21*(9), 1433–1436. https://doi.org/10.1029/WR021i009p01433

Karasaki, K., Long, J., & Witherspoon, P. (1988). Analytical models of slug tests. *Water Resources Research*, *24*(1), 115–126. https://doi.org/10.1029/WR024i001p00115

Kim, N. (2003). Remarks for the axisymmetric Navier–Stokes equations. *Journal of Differential Equations*, *187*(2), 226–239. https://doi.org/10.1016/S0022-0396(02)00077-3

Kipp, K. L. Jr. (1985). Type curve analysis of inertial effects in the response of a well to a slug test. *Water Resources Research*, *21*(9), 1397–1408. https://doi.org/10.1029/WR021i009p01397

Koh, E.-H., Lee, E., & Lee, K.-K. (2016). Impact of leaky wells on nitrate cross-contamination in a layered aquifer system: Methodology for and demonstration of quantitative assessment and prediction. *Journal of Hydrology*, *541*, 1133–1144. https://doi.org/10.1016/j.jhydrol.2016.08.019

Lacombe, S., Sudicky, E., Frape, S., & Unger, A. (1995). Influence of leaky boreholes on cross-formational groundwater flow and contaminant transport. *Water Resources Research*, *31*(8), 1871–1882. https://doi.org/10.1029/95WR00661

Liang, X., Zhan, H., & Zhang, Y. K. (2018). Aquifer recharge using a vadose zone infiltration well. *Water Resources Research*, *54*, 8847–8863. https://doi.org/10.1029/2018WR023409

Maji, R., & Sudicky, E. (2008). Influence of mass transfer characteristics for DNAPL source depletion and contaminant flux in a highly characterized glaciofluvial aquifer. *Journal of Contaminant Hydrology*, *102*(1–2), 105–119. https://doi.org/10.1016/j.jconhyd.2008.08.005

Malama, B., Kuhlman, K. L., Barrash, W., Cardiff, M., & Thoma, M. (2011). Modeling slug tests in unconfined aquifers taking into account water table kinematics, wellbore skin and inertial effects. *Journal of Hydrology*, *408*(1–2), 113–126. https://doi.org/10.1016/j.jhydrol.2011.07.028

Malama, B., Kuhlman, K. L., Brauchler, R., & Bayer, P. (2016). Modeling cross-hole slug tests in an unconfined aquifer. *Journal of Hydrology*, *540*, 784–796. https://doi.org/10.1016/j.jhydrol.2016.06.060

Malvern, L. E. (1969). *Introduction to the mechanics of a continuous medium*. Englewood Cliffs: Prentice-Hall.

Marschall, P., & Barczewski, B. (1989). The analysis of slug tests in the frequency domain. *Water Resources Research*, *25*(11), 2388–2396. https://doi.org/10.1029/WR025i011p02388

McElwee, C. (2002). Improving the analysis of slug tests. *Journal of Hydrology*, *269*(3–4), 122–133. https://doi.org/10.1016/S0022-1694(02)00214-7

McElwee, C., Bohling, G., & Butler, J. Jr. (1995). Sensitivity analysis of slug tests. Part 1. The slugged well. *Journal of Hydrology*, *164*(1–4), 53–67. https://doi.org/10.1016/0022-1694(94)02568-V

McElwee, C., Butler, J. J. Jr., Bohling, G., & Liu, W. (1995). Sensitivity analysis of slug tests Part 2. Observation wells. *Journal of Hydrology*, *164*(1–4), 69–87. https://doi.org/10.1016/0022-1694(94)02569-W

McElwee, C., & Zenner, M. (1998). A nonlinear model for analysis of slug-test data. *Water Resources Research*, *34*(1), 55–66. https://doi.org/10.1029/97WR02710

Melville, J. G., Molz, F. J., Güven, O., & Widdowson, M. A. (1991). Multilevel slug tests with comparisons to tracer data. *Groundwater*, *29*(6), 897–907. https://doi.org/10.1111/j.1745-6584.1991.tb00577.x

Paradis, D., Gloaguen, E., Lefebvre, R., & Giroux, B. (2015). Resolution analysis of tomographic slug test head data: Two-dimensional radial case. *Water Resources Research*, *51*, 2356–2376. https://doi.org/10.1002/2013WR014785

Quinn, P., Klammler, H., Cherry, J., & Parker, B. (2018). Insights from unsteady flow analysis of underdamped slug tests in fractured rock. *Water Resources Research*, *54*, 5825–5840. https://doi.org/10.1029/2018WR022874

Ramey, H. J., Agarwal, R. G., & Martin, I. (1975). Analysis of "slug test" or DST flow period data. *Journal of Canadian Petroleum Technology*, *14*(03). https://doi.org/10.2118/75-03-04

Shapiro, A. M., & Hsieh, P. A. (1998). How good are estimates of transmissivity from slug tests in fractured rock? *Groundwater*, *36*(1), 37–48. https://doi.org/10.1111/j.1745-6584.1998.tb01063.x

Springer, R., & Gelhar, L. (1991). Characterization of large-scale aquifer heterogeneity in glacial outwash by analysis of slug tests with oscillatory response, Cape Cod, Massachusetts. *U.S. Geological Survey Toxic Substance Hydrology Program: Proceedings of the Technical Meeting, Monterey, California*, *91*, 36–40. https://doi.org/10.3133/wri914034

Van der Kamp, G. (1976). Determining aquifer transmissivity by means of well response tests: The underdamped case. *Water Resources Research*, *12*(1), 71–77. https://doi.org/10.1029/WR012i001p00071

Wang, X., Jourde, H., Aliouache, M., & Massonnat, G. (2018). Characterization of horizontal transmissivity anisotropy using cross-hole slug tests. *Journal of Hydrology*, *564*, 89–98. https://doi.org/10.1016/j.jhydrol.2018.06.068

Widdowson, M. A., Molz, F. J., & Melville, J. G. (1990). An analysis technique for multilevel and partially penetrating slug test data. *Groundwater*, *28*(6), 937–945. https://doi.org/10.1111/j.1745-6584.1990.tb01730.x

Yang, L., Wang, X. S., & Jiao, J. J. (2015). Numerical modeling of slug tests with MODFLOW using equivalent well blocks. *Groundwater*, *53*(1), 158–163. https://doi.org/10.1111/gwat.12181

Zenner, M. A. (2008). Experimental evidence of the applicability of Colebrook and Borda Carnot-type head loss formulas in transient slug test analysis. *Journal of Hydraulic Engineering*, *134*(5), 644–651. https://doi.org/10.1061/(ASCE)0733-9429(2008)134:5(644)

Zhu, J., & Yeh, T.-C. J. (2005). Characterization of aquifer heterogeneity using transient hydraulic tomography. *Water Resources Research*, *41*, W07028. https://doi.org/10.1029/2004WR003790

Zlotnik, V. A., & McGuire, V. L. (1998). Multi-level slug tests in highly permeable formations: 1. Modification of the Springer-Gelhar (SG) model. *Journal of Hydrology*, *204*(1–4), 271–282. https://doi.org/10.1016/S0022-1694(97)00128-5

Zurbuchen, B. R., Zlotnik, V. A., & Butler, J. J. Jr. (2002). Dynamic interpretation of slug tests in highly permeable aquifers. *Water Resources Research*, *38*(3), 7-1-7-18. https://doi.org/10.1029/2001WR000354